Electronic Supplementary Information

Development of multifunctional ionogels derived from a dynamic deep eutectic solvent

Jintao Li, Mingzu Zhang, Jinlin He* and Peihong Ni

College of Chemistry, Chemical Engineering and Materials Science, State and Local Joint Engineering Laboratory for Novel Functional Polymeric Materials, Jiangsu Key Laboratory of Advanced Functional Polymer Design and Application, Suzhou Key Laboratory of Macromolecular Design and Precision Synthesis, Soochow University, Suzhou, Jiangsu, 215123, P. R. China. E-mail: jlhe@suda.edu.cn

Experimental Section

Chemicals

Choline chloride (ChCl, 99%) and (±)-α-lipoic acid (LA, 99%) were purchased from Adamas. Tannic acid (TA, A.R.) was purchased from Macklin. 1,3-diisopropenylbenzene (DIB, 97%) and aluminum chloride hexahydrate ($AlCl_3 \cdot 6H_2O$, 99%) were purchased from Aladdin. The other chemicals were obtained from Jiangsu Chinasun Specialty Products Co.. All the reagents were used as received.

Synthesis of DDES-based ionogels

The ionogels were prepared by the combination of one-step ring-opening polymerization (ROP) and dynamic interactions. ChCl (1.0 g) and LA (5.0 g) were first added to a 50 mL round-bottom flask with a stirrer, and stirred at 120 °C for 1 h to obtain an

orange-yellow transparent dynamic deep eutectic solvent (DDES) in the molten state. TA (0.1 g, dissolved in 0.3 mL anhydrous ethanol) was then slowly added to the molten solution and stirred for 20 min at the same temperature until achieving well mixing. Next, DIB (0.5 g) was added dropwise to the molten solution and stirred for 20 min. Finally, $AlCl_3{\cdot}6H_2O$ (0-1.6 *wt.*%, mass ratio compared with the LA, dissolved in 0.3 mL anhydrous ethanol) was added to the above mixture and stirred for 20 min. The resulting mixture was poured into a PTFE mold and placed in an oven at 35 °C for 24 h to obtain a yellow transparent ionogel. A series of DDES-based ionogel ($PDDES_x$) were prepared by varying the feeding content of the $AlCl_3{\cdot}6H_2O$, in which x denotes the mass ratio of $AlCl_3{\cdot}6H_2O$ as compared with the LA content. For comparison, the $PDDES_{DIB}$ ionogel was also synthesized with the addition of DIB only.

General characterizations

Fourier transform infrared (FT-IR) spectra were recorded using a spectrometer (Vertex 70, Bruker). Attenuated total reflectance (ATR) mode was used to scan 32 times with a scanning range of 600-4000 cm^{-1} and a spectral resolution of 4 cm^{-1}. Raman spectra were recorded by using a confocal micro Raman spectrometer (HR-800, Jobin Yvon) at an excitation wavelength of 785 nm with 32 scans in the range of 200-4000 cm^{-1} and a spectral resolution of 1 cm^{-1}. X-ray diffraction (XRD, D8 Advance, Bruker) analysis was performed at room temperature (25±1 °C) with 2θ range of 5-50°. The transparency of the sample over the 400-800 nm range was measured using a UV-Vis spectrophotometer (UV-3600, Shimadzu). The surface morphology and elemental composition of the raw materials and samples were characterized using a cold field emission scanning electron microscope & energy spectrometer (SEM-EDS, SU-8010, Hitachi). Thermogravimetric analysis (TGA) was performed on an instrument (Discovery, TA) with about 5 mg sample in the platinum plate. Beginning with equilibrating at 30 °C, the temperature was ramped from 30 to 600 °C at a heating rate of 10 °C min^{-1} under a nitrogen atmosphere. Differential scanning calorimeter (DSC) curves were obtained by the DSC2010 instrument (TA) from -20 to 150

°C at a heating rate of 10 °C min^{-1} with a 1 min isothermal hold at the maximum and minimum temperatures. All glass transition temperatures (T_g) or melting temperature (T_m) of samples were reported according to the second heating scans. The rheological experiments were performed by rotational rheometer (RS6000; Thermo Fisher Scientific). The time sweep was performed from 0 s to 120 s with 1% strain. The frequency sweep was conducted in the frequency ranges of 0.1 to 100 rad s^{-1} with a constant strain of 1%. The dynamic strain sweep was measured from 0.1% to 1000% at a frequency of 6.28 rad s^{-1}.

Mechanical tests

All the mechanical tests were carried out at room temperature using a tensile testing machine (Instron 5965, 5 kN load cell). Each sample was rectangular in shape (length: 40 mm, width: 20 mm, thickness: 1 mm). For the tensile test, the distance between the clamps was 20 mm and the stretching rate was set as 50 mm min^{-1}. For the compression test, the samples were cylindrical, with a height of 10 mm and a diameter of 10 mm. The compression rate was set as 25 mm min^{-1}. The data were recorded in real time by a connected computer. Each mechanical value was calculated from the average value of three measurements.

Self-healing tests

The PDDES ionogels (40 mm×20 mm×1 mm) were cut into two identical pieces with a knife and then placed in an oven at 35 °C to contact them at different healing times without any additional stimulation. The self-healing morphology of the ionogel was observed using an optical microscope (Phoenix, PH100-3B41L-IPL). A universal tensile testing machine (Instron 5965, 5 kN load cell) was used to test the healed samples in tension at a rate of 50 mm min^{-1} and stress-strain curves were obtained for the healed samples. The self-healing efficiency (SHE) was calculated from the ratio of the tensile strain at break of the healed sample to the tensile strain at break of the original sample.

Adhesion tests

The PDDES ionogels were cut into rectangular shapes (20 mm×20 mm×1 mm), and placed between two glass slides, or the other substrates such as paper, Fe and plastic. The

samples were evenly distributed between two identical substrates with an overlapped area of about 4 cm^2, and then pressed by hand for approximately 1 min. A universal tensile tester (Instron 5965, 5 kN load cell) was used to perform the lap shear test, where the two slides were clamped between two jigs in a vertical direction, and the rate of stretching was set as 20 mm min^{-1}. The data was recorded in real time by a connected computer. The adhesion strength (F_a) is calculated according to the following formula (1), where F_m is the maximum tensile stress and S is the contact area between the sample and the substrate. At least three sets of samples were tested for each substrate and the adhesion strength was calculated based on the average of three measurements.

$$F_a = \frac{F_m}{S} \tag{1}$$

Recycling process

The recovery process simply involved heating the fractured PDDES ionogel at 120 °C for 10 min until the solid ionogel was completely melted into a homogeneous slight red and clear liquid. The recovered liquid was then poured into a PTFE mold and kept in an oven at 35 °C for 24 h to obtain the recycled PDDES.

Electrical tests

The ionic conductivity of PDDES ionogels was measured by the bulk resistance (R_b), which was determined by the electrochemical impedance spectroscopy (EIS) on the electrochemical workstation (CHI660c, Shanghai Chenhua Instruments) from 1 Hz to 100 kHz. The blocking cell (SS/PDDES/SS) was assembled by a PDDES ionogel and two symmetric stainless steels electrodes (SS, Φ=14 mm), and the ionic conductivity (σ) was calculated according to the following formula (2), where d (cm), R_b (Ω) and S (cm^2) are the thickness, bulk impendence and contact area of PDDES ionogel, respectively.

$$\sigma = \frac{d}{R_b \times S} \tag{2}$$

The electrical self-healing and sensing performance of the PDDES ionogel was tested using an LCR digital bridge tester (TH2830, Changzhou Tonghui Electronics). Copper wires

were connected to each end of the ionogel (40 mm×20 mm×1 mm) and the other end of the copper wire was connected to the test apparatus, which was subjected to cyclic tensile sensing tests using a universal tensile tester (Instron 5965, 5 kN load cell) and the change in relative resistance signal with strain was recorded in real time. Similarly, the ionogel with the same size was used to assemble a wearable sensor to detect finger joint movements. The ends of the ionogel were connected to copper wires, which were then attached directly to the volunteer's knuckles and secured with 3M tape to sense their movements, and the signal changes were recorded in real time using the tester described above. The change in relative resistance signal ($\Delta R/R_0$) is calculated according to the following formula (3), where R is the resistance of the ionogel in the stretched state and R_0 is the resistance of the ionogel in the original state. The gauge factor (GF) is calculated to assess the strain sensing sensitivity of the ionogels according to the following formula (4), where ΔL is the change in stretch length and L_0 is the original length.

$$\Delta R/R_0 = \left(R\text{-}R_0\right)/R_0 \times 100\% \tag{3}$$

$$\mathrm{GF}=\left(\frac{\Delta R/R_0}{\Delta L/L_0}\right) \tag{4}$$

Table S1 Compositions and contents of DDES-based ionogels (PDDES).

Sample	ChCl (g)	LA (g)	TA (g)	DIB (g)	$AlCl_3 \cdot 6H_2O$ (g)
$PDDES_{DIB}$	1.0	5.0	0	0.5	0
$PDDES_0$			0.1		0
$PDDES_{0.2}$					0.01
$PDDES_{0.4}$					0.02
$PDDES_{0.8}$					0.04
$PDDES_{1.6}$					0.08

Table S2 Summary of uniaxial tensile data of PDDES ionogels.

Sample	Stress at break (kPa)	Strain at break (%)	Young' modulus (kPa)	Toughness (kJ m^{-3})	Fracture energy (kJ m^{-2})
$PDDES_{0.2}$	85±4	1270±27	91±2	715±21	11±0.9
$PDDES_{0.4}$	110±9	1060±191	95±10	673±139	11±1.2
$PDDES_{0.8}$	166±5	887±13	107±13	598±39	12±0.2
$PDDES_{1.6}$	266±25	672±23	147±4	780±73	14±1.7

In Fig. S1a, a solid mixture with precipitated particles is formed in the ChCl/LA/TA and ChCl/LA/Al^{3+} groups, indicating that the ring-closing depolymerization may not be well inhibited by adding TA or Al^{3+} alone. In addition, although the ChCl/LA/DIB group ($PDDES_{DIB}$) formed a homogeneous material, its mechanical properties were much weaker than those of the ChCl/LA/TA/DIB/Al^{3+} PDDES.

As shown in Fig. S1b, ChCl and LA were made eutectic at a heating temperature of 120 °C while undergoing ring-opening polymerization to form a sub-stable dynamic DES. TA, DIB and $AlCl_3$ were then sequentially added to the liquid molten DDES to obtain the PDDES ionogel via a one-pot method. In this system, ChCl was locked in the polymer network through hydrogen bonding and could provide charge carriers along the polymer chain. The natural plant polyphenol TA acted as a free radical scavenger to inhibit the inverse ring-closing depolymerization reaction initiated by the reactive sulphur radicals at the end of the poly(LA) chain.[1,2] Meanwhile, DIB acted as a chemical cross-linking agent to further stabilize the polymer chain, thus preventing the polymer from forming a hard and opaque solid due to depolymerization.[3,4] The introduction of Al^{3+} could physically coordinate with the phenolic hydroxyl groups in TA and the carboxyl groups in the polymer chain to further endow the system with dynamic property and enhance the toughness of the cross-linked network. Thus, we successfully prepared a solid, transparent, soft and stable at room temperature DDES-based ionogel.

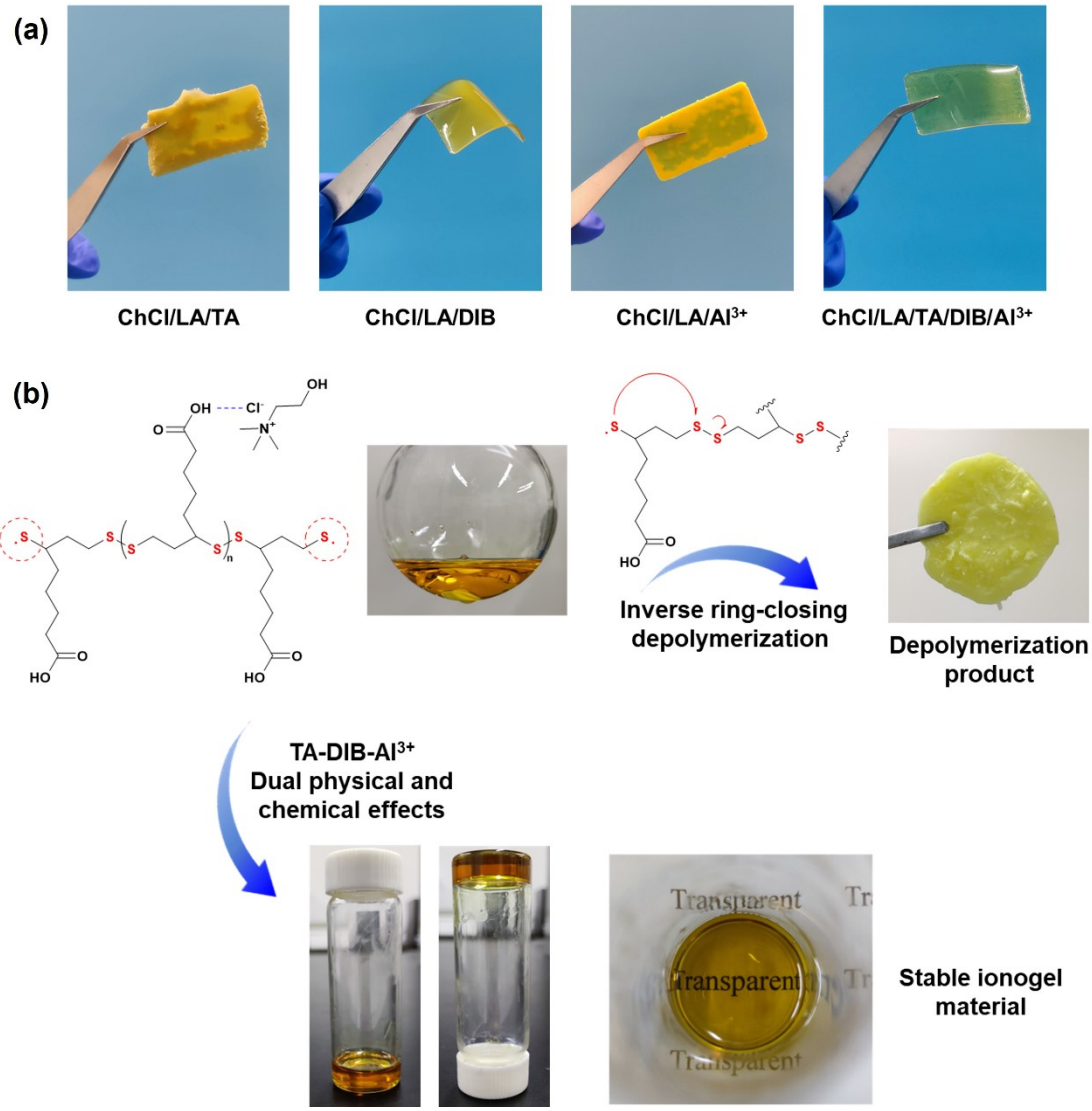

Fig. S1 (a) Photos of materials made from different components. (b) Inverse ring-closing depolymerization and inhibition of ionogels. The addition of TA and DIB inhibits the depolymerization reaction and delays the moisture absorption of the material.

As shown in Fig. 1a and Fig. S2, compared to the raw materials, the formation of hydrogen bonds within the ionogel is observed at 3360 cm^{-1} in $PDDES_{0.2}$. The formation of hydrogen bond is further supported by the shift of the stretching vibration absorption peak attributed to the carbonyl group from 1688 to 1700 cm^{-1}. A clear internal carboxyl-Al^{3+} stretching vibrational absorption peak is observed at 1656 cm^{-1}, in addition to vibrational absorption peaks attributed to S-Ar at 1046 cm^{-1} and S-CH_2 at 1200 cm^{-1}, suggesting that the sulphur radicals formed during LA ring opening successfully react with the TA benzene ring and the double bond of DIB to form a cross-linked structure.[1,2,4]

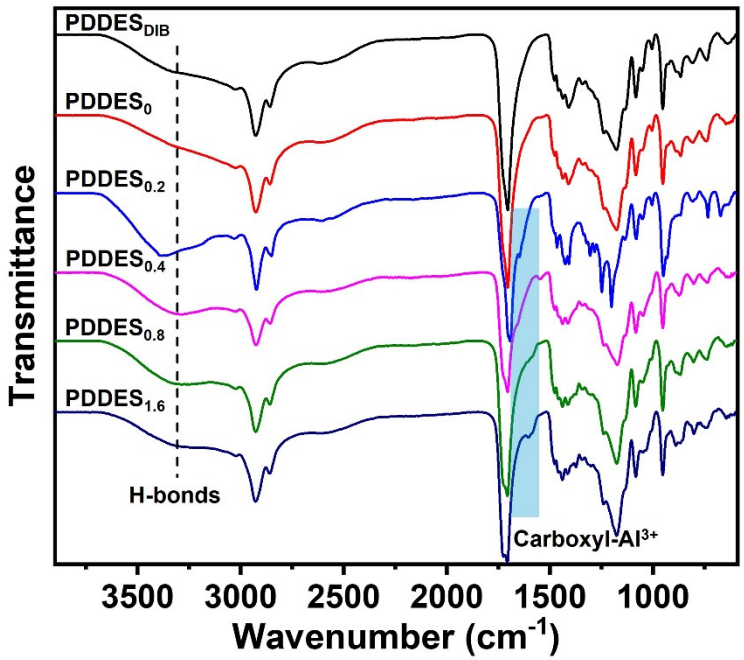

Fig. S2 FT-IR spectra of PDDES ionogels.

As shown in Fig. 1b and Fig. S3, the peak at 511 cm^{-1} is attributed to the disulfide bond, which split into two distinct peaks at 508 and 525 cm^{-1}, confirming the ring-opening polymerization of LA. In addition, the characteristic peaks attributed to C-S and C-C are observed at 673 and 1000 cm^{-1}, respectively, which further indicate that the exposed sulphur radicals were well quenched to avoid ring-closing depolymerization.[1,4]

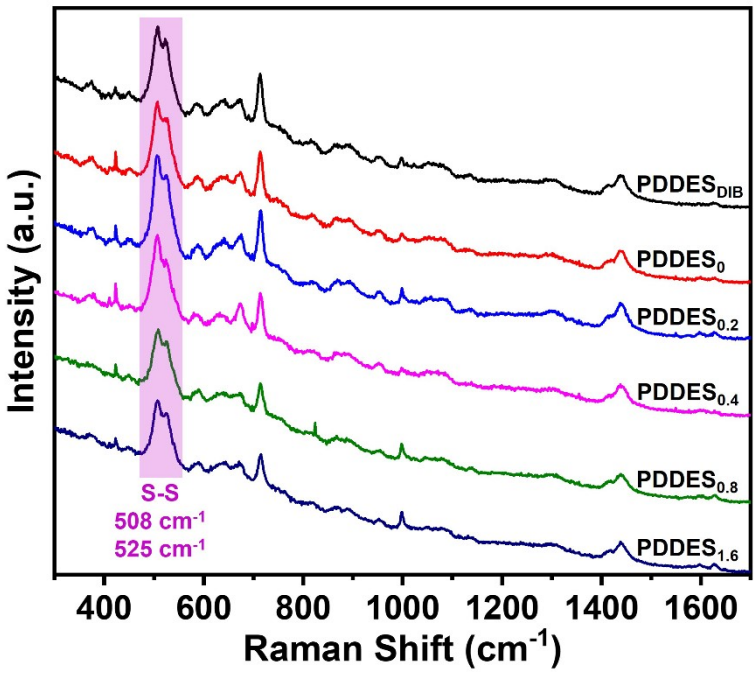

Fig. S3 Raman spectra of PDDES ionogels.

The XRD patterns were compared to confirm that LA was completely ring-opening polymerized to form amorphous polymer. As shown in Fig. 1c and Fig. S4, it can be found that the XRD pattern of LA molecule clearly shows strong crystalline diffraction, indicating that the internal structure of LA was dominated by the crystalline state. In contrast, all the PDDES ionogels show a small and broad peak at about 20°, demonstrating that the LA molecule has undergone ROP reaction to yield amorphous polymer.[2,4] Moreover, no other sharp peaks can be observed in the spectrum of ionogels, which indicated the absence of depolymerization.

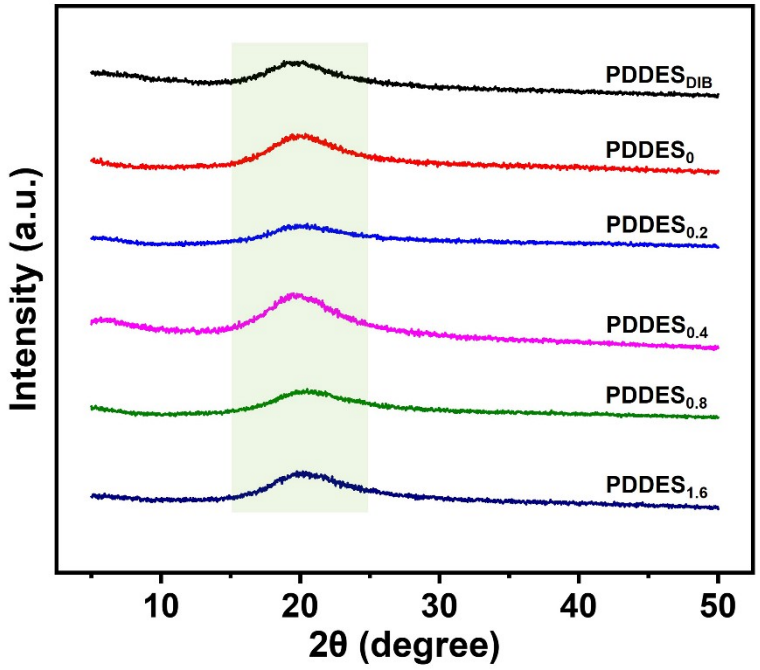

Fig. S4 XRD spectra of PDDES ionogels.

SEM analysis was used to visualize the microscopic surface morphology of LA, TA and $PDDES_{0.2}$, and the results are shown in Fig. S5. In comparison, it can be found that $PDDES_{0.2}$ shows a smooth morphology, which may be attributed to the presence of a stable cross-linked structure inside the ionogel leading to the formation of a dense network with good flexibility. In addition, the results of EDS analysis (Figs. S5 and S6) also show the uniform distribution of C, O, S, Cl and Al elements in the ionogel.

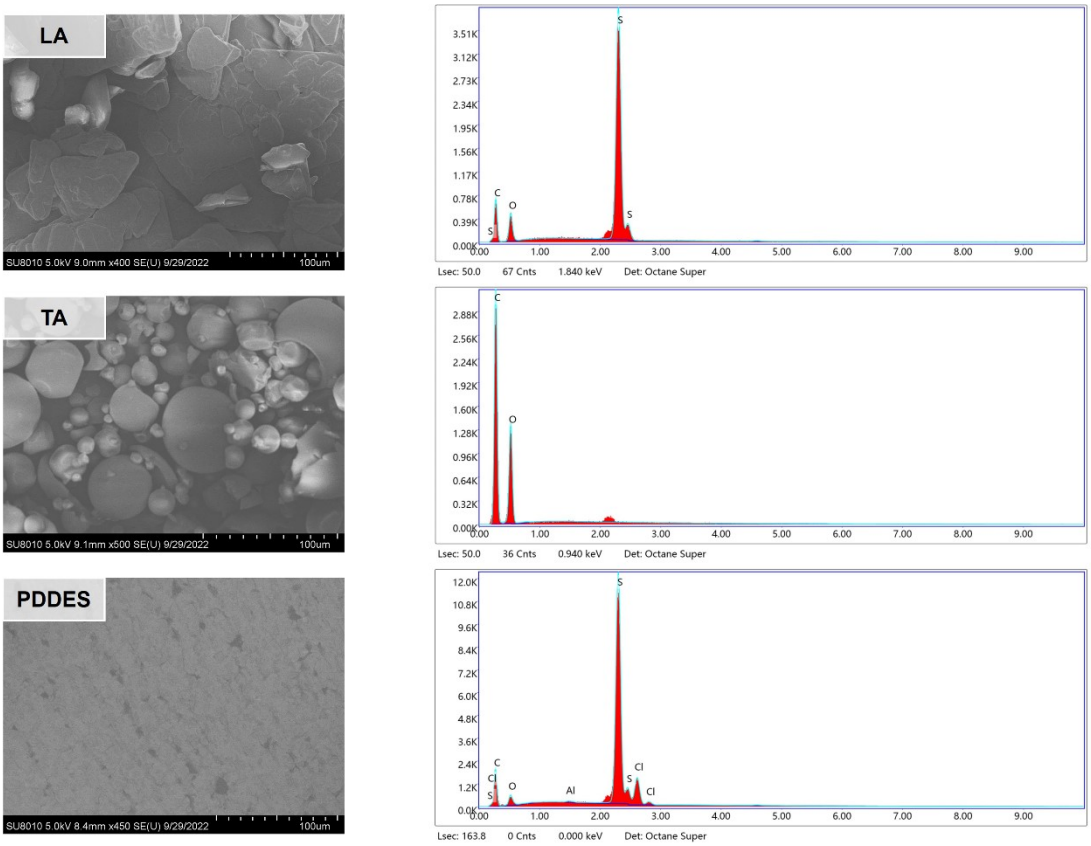

Fig. S5 SEM images and EDS analysis results of LA, TA and $PDDES_{0.2}$.

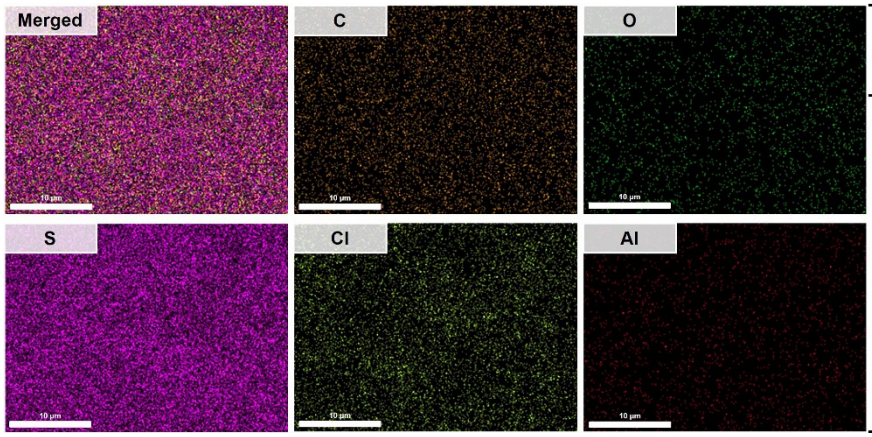

Element	Weight (%)	Atomic (%)
C	51.76	72.30
O	5.22	5.47
S	36.58	19.14
Cl	6.18	2.92
Al	0.27	0.17
Sum	100.01	100.00

Fig. S6 The element mapping images of $PDDES_{0.2}$ ionogel.

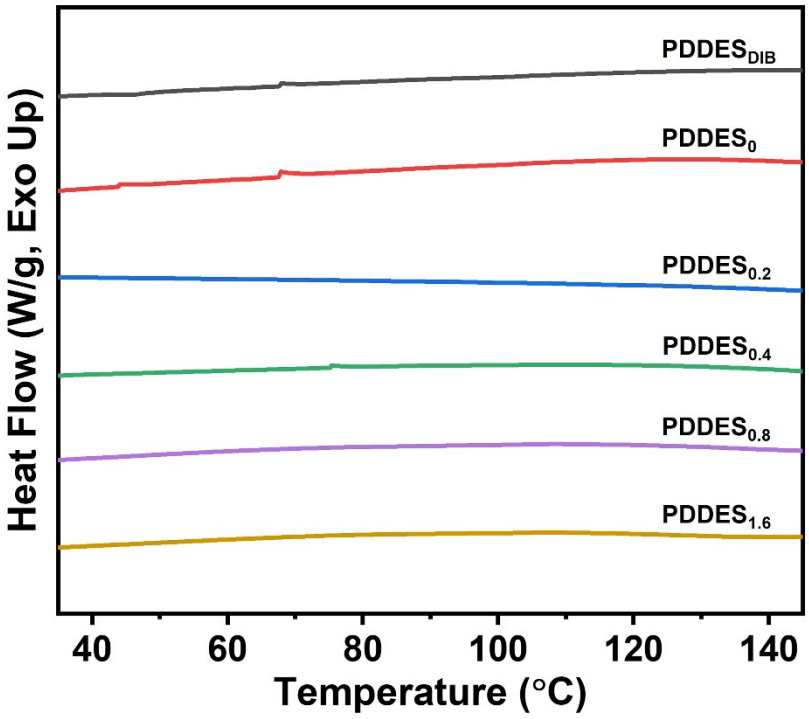

Fig. S7 DSC thermograms of PDDES ionogels.

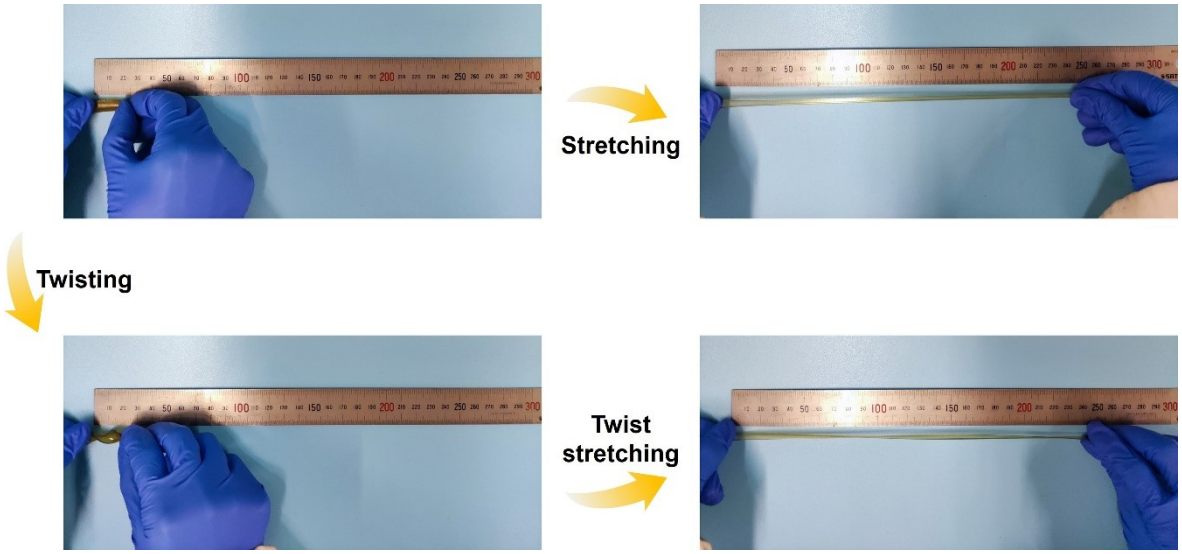

Fig. S8 Photos of $PDDES_{0.2}$ ionogel undergoing stretching and twist stretching.

Fig. S9a clearly shows the variation of the material fracture stress and elongation at break with increasing Al^{3+} content. The Young's modulus of the ionogel is observed to slightly increase with increasing Al^{3+} content from Fig. S9b, signifying a gradual increase in the stiffness of the material. In addition, the material exhibited a toughness close to 10^3 kJ m^{-3} and a fracture energy greater than 10 kJ m^{-2}, showing the characteristics of a typical ionogel with some potential in the application of flexible electronic devices.[5]

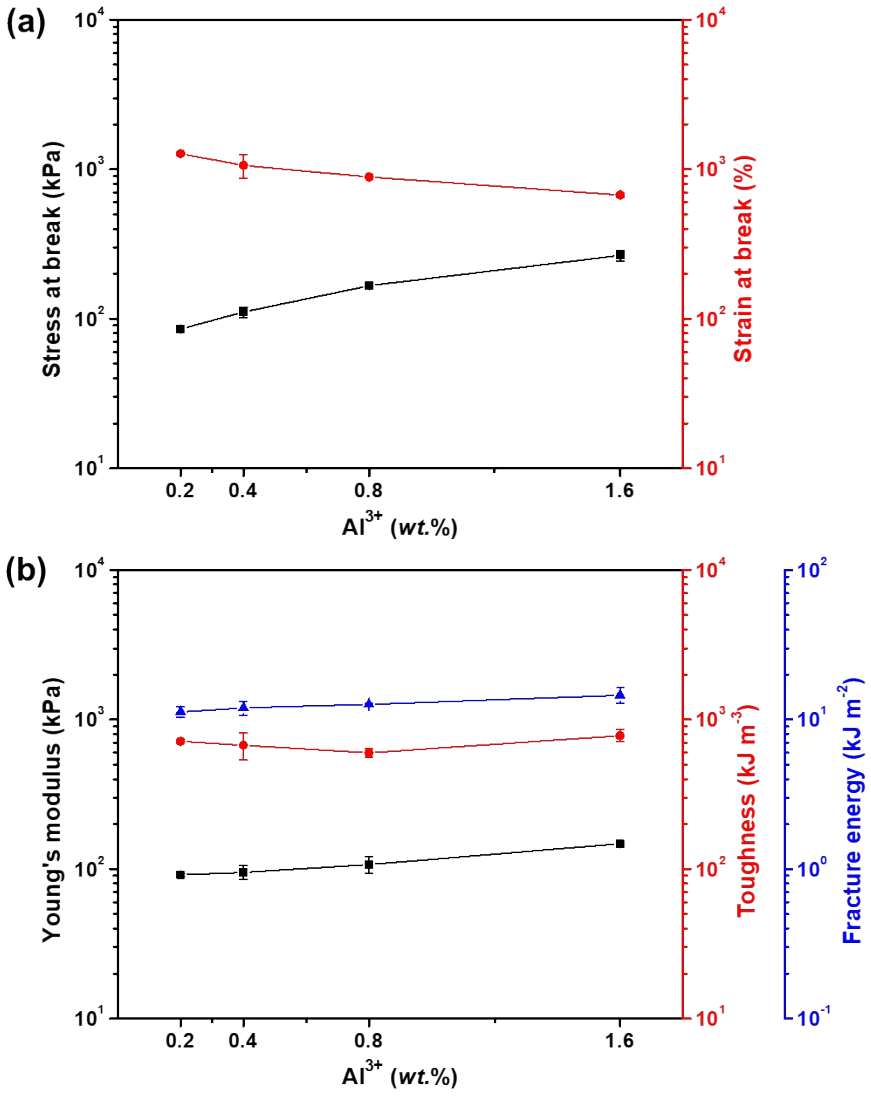

Fig. S9 (a) Stress and strain at ionogels fracture; (b) Young's modulus, toughness and fracture energy of ionogels.

The fatigue resistance of ionogel was further investigated by cyclic tensile tests. As shown in Figs. S10a and S10b, the material exhibited a larger energy dissipation in a shorter response time. In order to observe the ability of ionogel to resist energy dissipation through self-recovery dynamic bonding, we performed cyclic tensile tests of $PDDES_{0.2}$ at different time intervals at 300% strain. The results showed that the hysteresis loop formed became significantly smaller with the increase of the given recovery time. In particular, when the cycle interval was 20 min, it was clearly observed that the first and second hysteresis loops appeared to overlap, and the tensile strength also returned to the initial state (Fig. S10c). From the cyclic tensile test plots at different strains, one could see that the loading-unloading curves of the ionogel showed a more pronounced hysteresis return line as the strain increases (Fig. S10d), indicating that the ionogel material could form an effective energy dissipation pathway through multiple dynamic bonding interactions (disulfide, hydrogen, and coordination bonds) internally. The dissipation mechanism may be that after the material was stretched, the transient network formed by non-covalent hydrogen bond was preferentially broken. Then, the metal-ligand, disulfide and double bond cross-linked networks started to break reversibly. When released, the triple dynamic bonds recombined to restore the integrity of the polymer network, thus ensured the excellent elasticity and fatigue resistance of ionogel.[6]

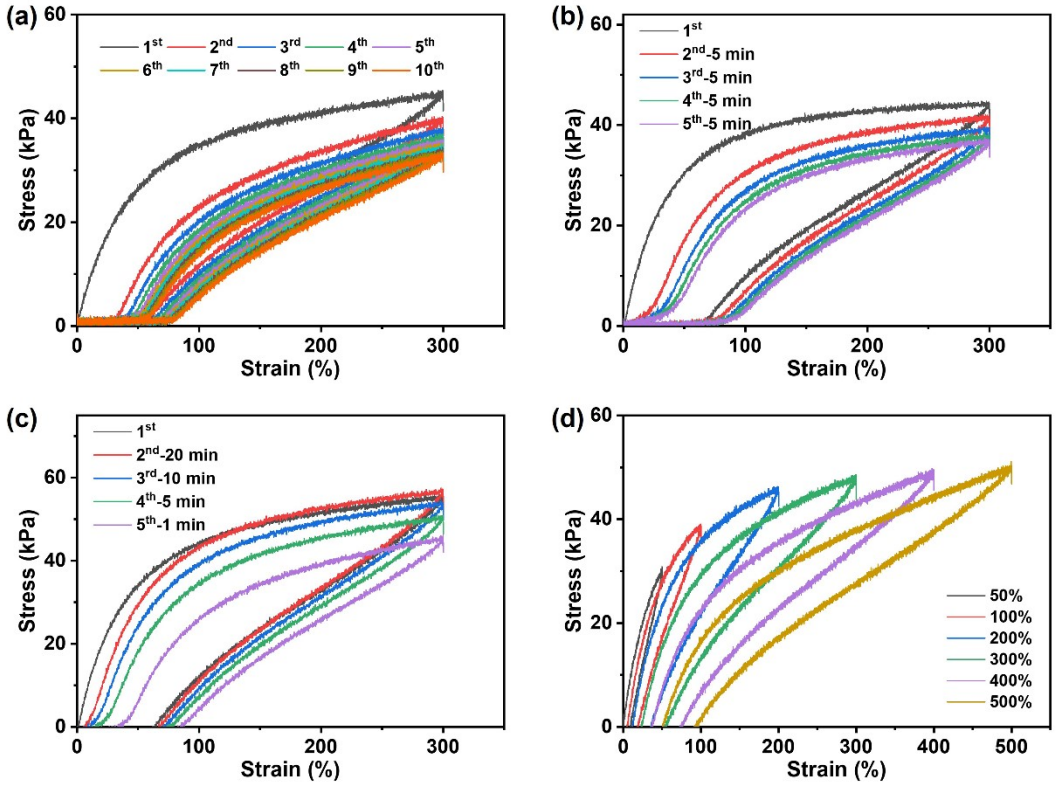

Fig. S10 Cyclic recovery curves of $PDDES_{0.2}$ ionogel measured by cyclic tensile tests. (a) Without intervals, (b) with 5 min intervals, (c) with 20, 10, 5, and 1 min intervals and (d) with different strains.

Rheological analysis was performed on ionogels to characterize their viscoelasticity. Fig. S11a shows the curves of storage modulus (G′) and loss modulus (G″) of PDDES at room temperature with time, and it's observed that G′ was dominated and significantly higher than G″, which indicated that the material had an elastic solid phase behavior. In addition, as the Al^{3+} content increased from 0 to 1.6 *wt.*%, the G′ and G″ of the polymer network were significantly enhanced, indicating that the metal coordination bond had a contribution to the strength of the polymer network. The rheological results of the modulus variation with frequency for the $PDDES_{0.2}$ are shown in Fig. S11b, and G′ was higher than G″ in the frequency range of 0.1-100 rad s^{-1}, which further indicated that the material had a typical elastic solid network. From Fig. S11c, one can observe that the G′ of $PDDES_{0.2}$ was always larger than G″ in the strain range of 0.1%-1000%, demonstrating that the ionogel system had good elasticity in the large strain range without shifting toward the sol. In addition, the G″ value decreased slightly with the increase of shear strain, which may be related to the dissociation of disulfide, hydrogen, and coordination bonds in the polymer network.[7]

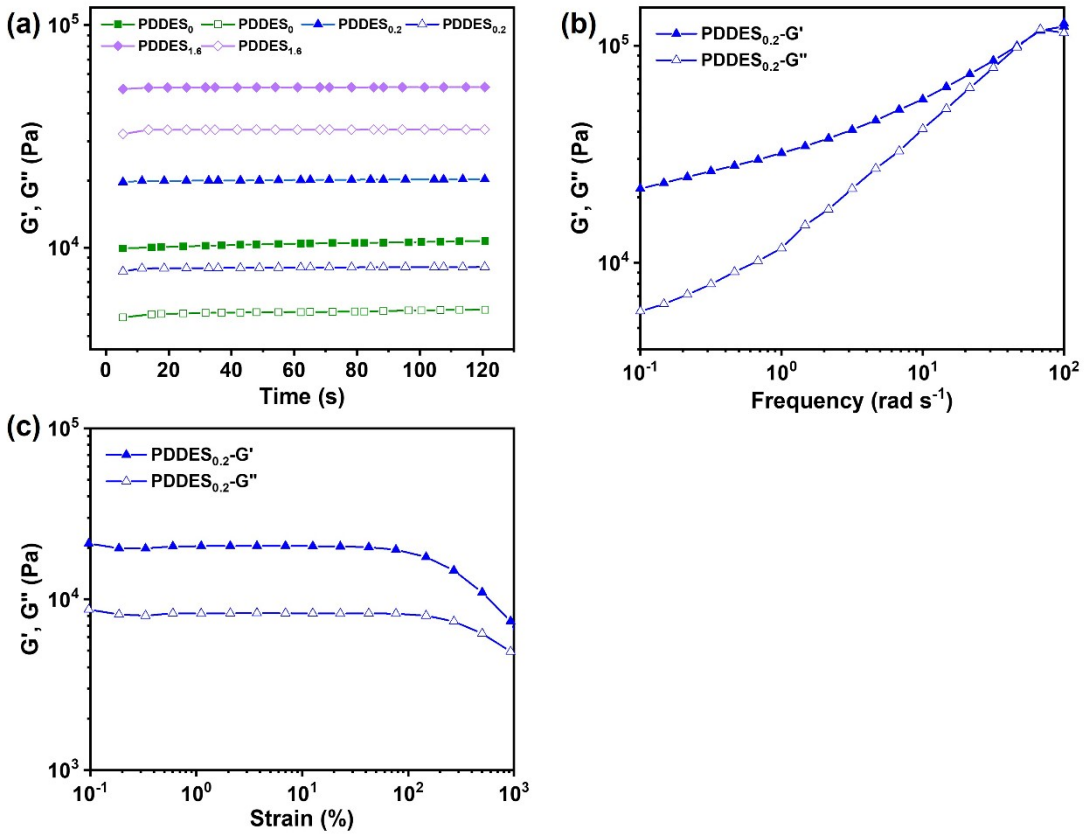

Fig. S11 (a) Time dependency of G′ (solid) and G″ (hollow) of ionogels with different Al^{3+} contents at 25 ℃. (b) Frequency dependency of G′ and G″ of $PDDES_{0.2}$ ionogel by 1% strain at 25 ℃. (c) Strain dependency of G′ and G″ of $PDDES_{0.2}$ ionogel by frequency of 6.28 rad s^{-1} at 25 ℃.

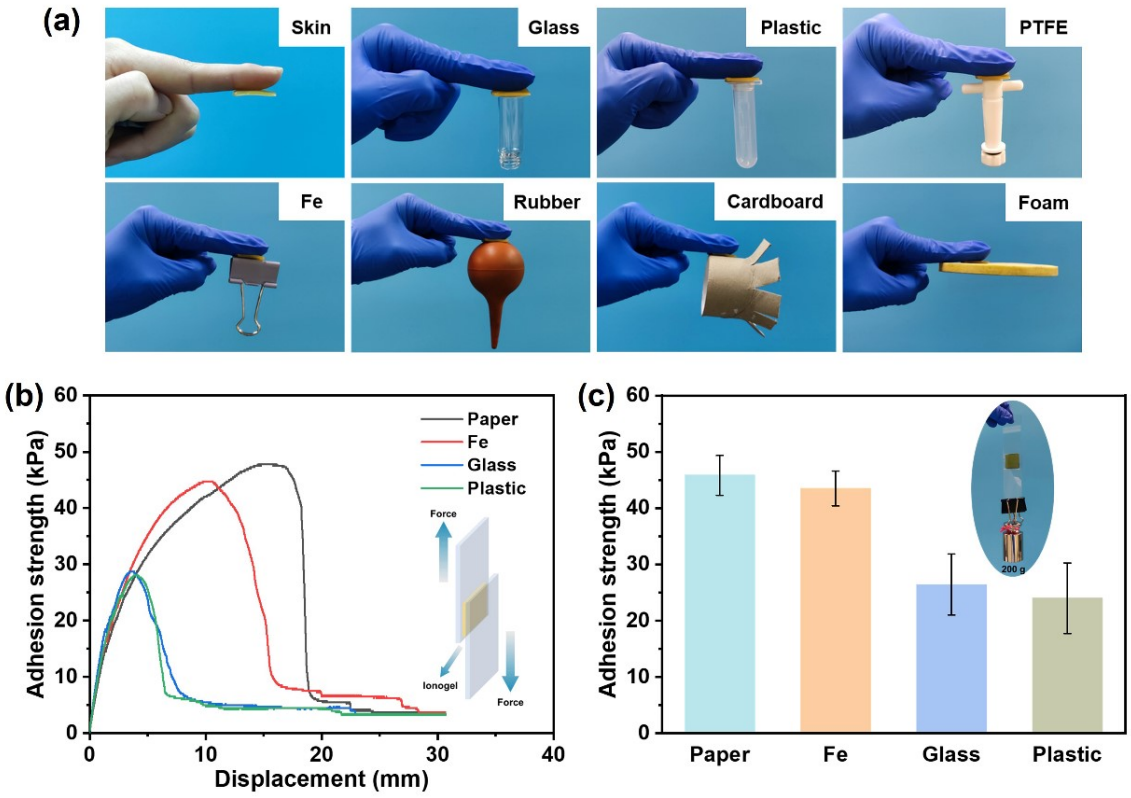

Fig. S12 (a) Adhesion photos of $PDDES_{0.2}$ on different substrate surfaces. (b) Adhesion curves based on lap-shear tests. (c) Adhesion strengths of $PDDES_{0.2}$ on four typical substrate surfaces, the inset shows that the ionogel adhered to the glass can lift a 200 g weight.

This stable adhesion to various substrates may be due to the presence of abundant hydroxyl, carboxyl and amphoteric groups in the gel network structure, which could form strong hydrogen bonds, metal-ligand bonds or electrostatic interactions at the interface, while the multiple interactions synergistically made them exhibit excellent adhesion properties. As shown from Fig. S13, the presence of a large number of carboxyl groups in the ionogel system promoted strong adhesion due to the easy hydrogen bonding in contact with the polyhydroxy surface of the paper; the good adhesion to metals could be attributed to the synergistic effect of surface adsorption and metal ligand complexation; the hydroxyl and Si-O groups on the surface of the glass would produce a large number of hydrogen bonds with the gel as well as electrostatic interactions; van der Waals interaction existed between the plastic and the ionogel; the F atoms of PTFE, and the phenolic hydroxyl groups of cellulose-based materials would produce high-density hydrogen bonds with the carboxyl and hydroxyl groups of the gel; the complex protein composition in skin tissue formed hydrogen bonds and π-π stacking interactions with ionogel thereby promoting good adhesion.[2,8-10] The excellent adhesion exhibited by such DDES-based ionogel to a wide range of substrates is highly beneficial for their application in biosensing.

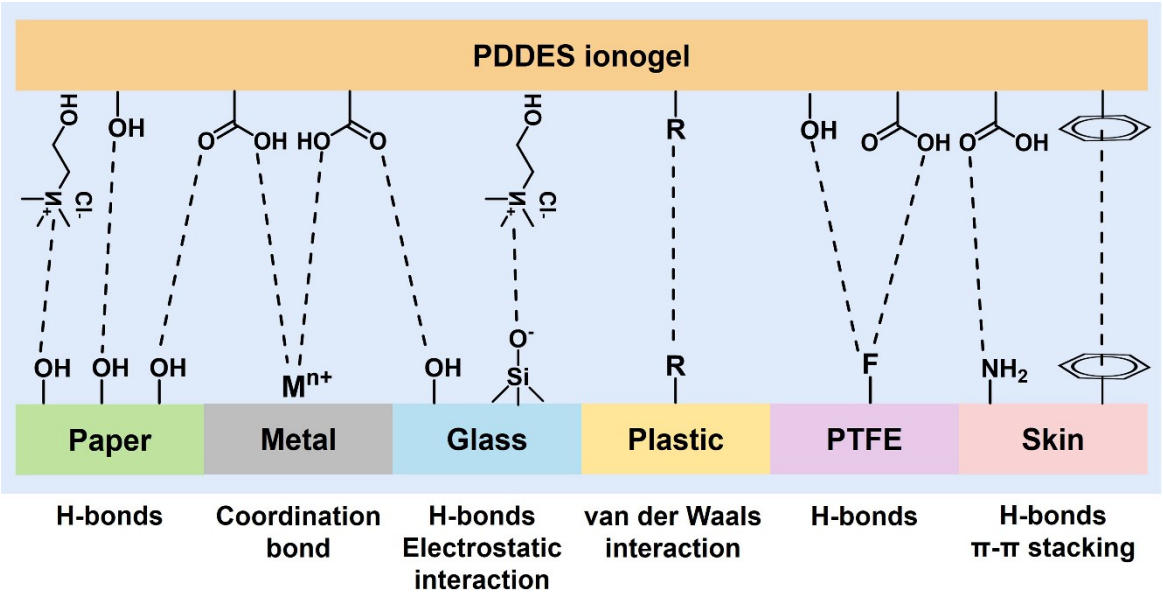

Fig. S13 Proposed adhesion mechanism of PDDES ionogel on different substrates.

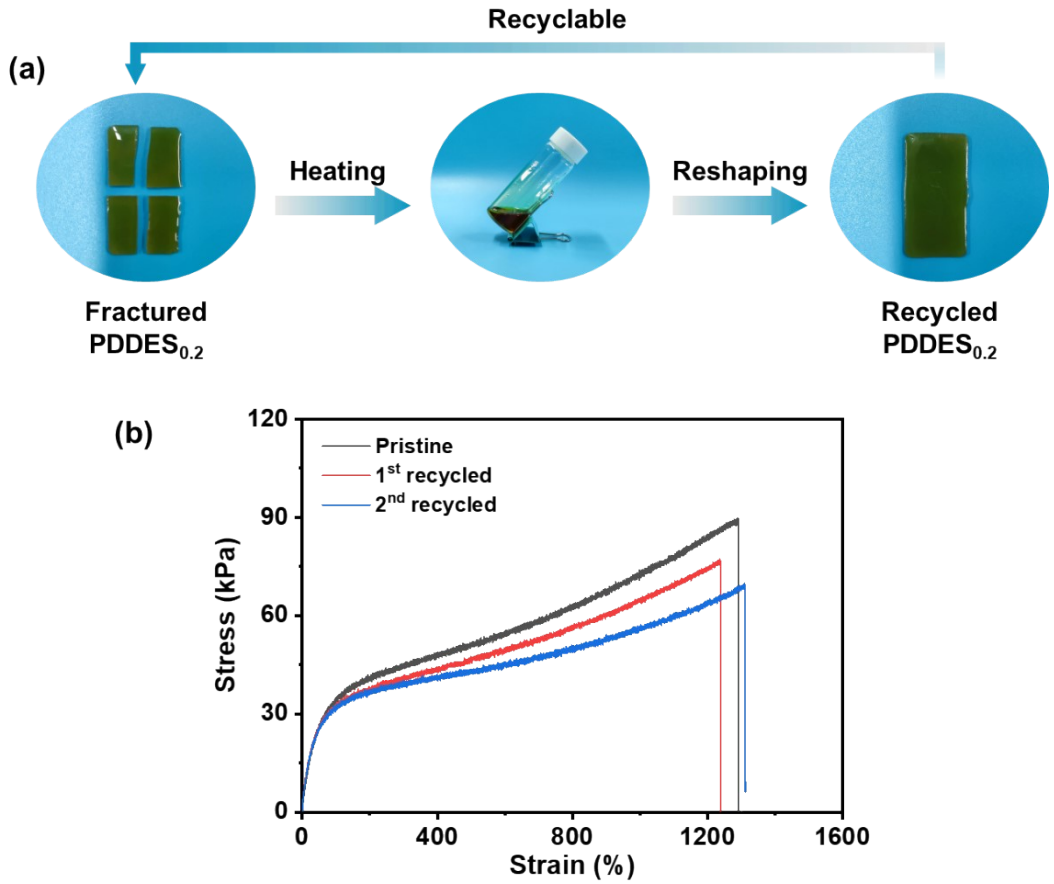

Fig. S14 (a) Schematic illustration of the recycling process of $PDDES_{0.2}$ ionogel. (b) stress-strain curves of pristine and recycled $PDDES_{0.2}$ ionogels.

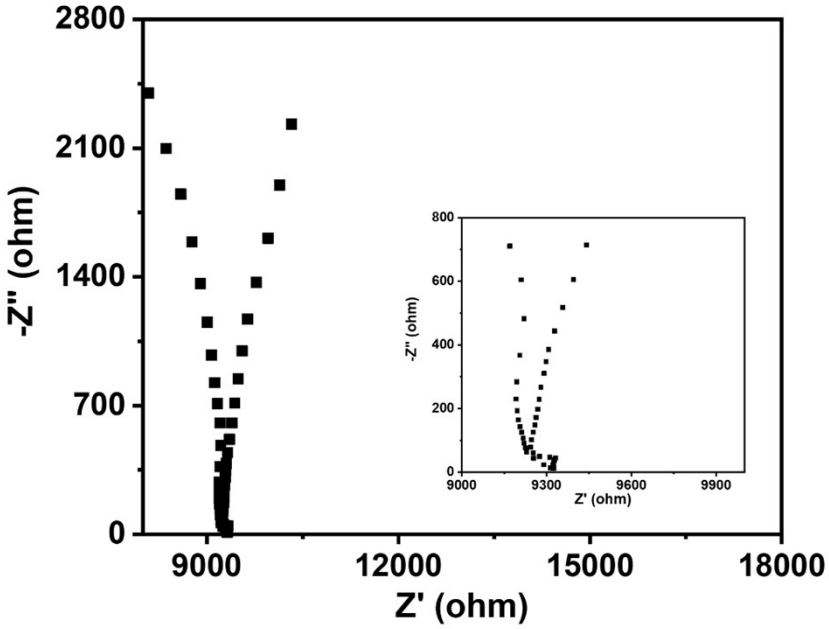

Fig. S15 Electrochemical impedance spectroscopy (EIS) plots of $PDDES_{0.2}$ ionogel.

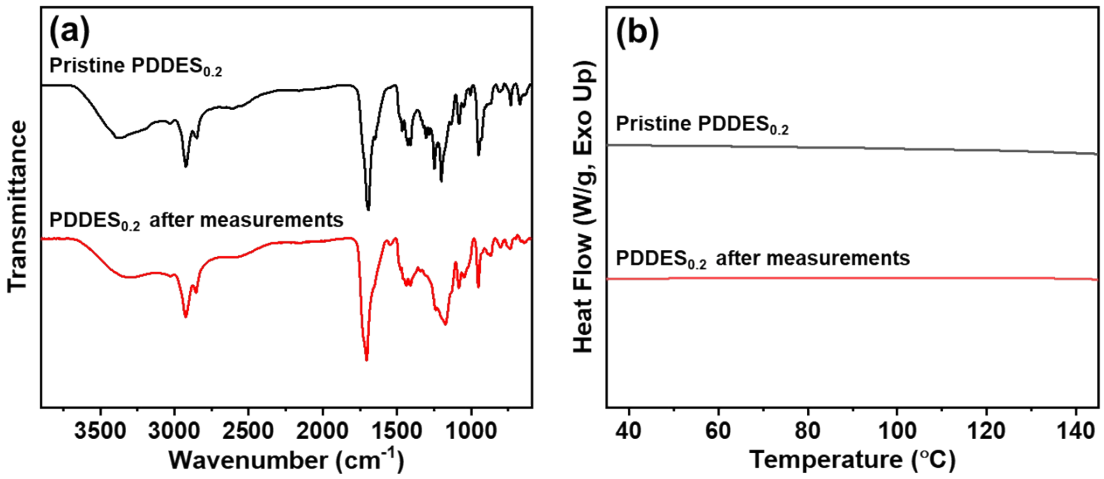

Fig. S16 (a) FT-IR spectra and (b) DSC thermograms of pristine $PDDES_{0.2}$ and $PDDES_{0.2}$ after the flexible conductor measurements.

References

1 C. Chen, X. Yang, S.-J. Li, C. Zhang, Y.-N. Ma, Y.-X. Ma, P. Gao, S.-Z. Gao and X.-J. Huang, *Green Chem.*, 2021, **23**, 1794-1804.

2 X. Ke, S. X. Tang, Z. Y. Dong, K. Ren, P. Yu, X. Y. Xu, J. J. Yang, J. Luo and J. S. Li, *Chem. Eng. J.*, 2022, **442**, 136206.

3 W. J. Chung, J. J. Griebel, E. T. Kim, H. Yoon, A. G. Simmonds, H. J. Ji, P. T. Dirlam, R. S. Glass, J. J. Wie, N. A. Nguyen, B. W. Guralnick, J. Park, Á. Somogyi, P. Theato, M. E. Mackay, Y. E. Sung, K. Char and J. Pyun, *Nat. Chem.*, 2013, **5**, 518-524.

4 Q. Zhang, C.-Y. Shi, D.-H. Qu, Y.-T. Long, B. L. Feringa and H. Tian, *Sci. Adv.*, 2018, **4**, eaat8192.

5 M. X. Wang, J. Hu and M. D. Dickey, *JACS Au*, 2022, **2**, 2645-2657.

6 C. Dang, F. Peng, H. C. Liu, X. Feng, Y. Liu, S. N. Hu and H. S. Qi, *J. Mater. Chem. A*, 2021, **9**, 13115-13124.

7 C. Dang, M. Wang, J. Yu, Y. Chen, S. H. Zhou, X. Feng, D. T. Liu and H. S. Qi, *Adv. Funct. Mater.*, 2019, **29**, 1902467.

8 L. Wang, S. J. Liu, J. J. Cheng, Y. Peng, F. F. Meng, Z. Q. Wu and H. Chen, *Soft Matter*, 2022, **18**, 6115-6123.

9 E. Feng, X. Li, X. Q. Li, M. Z. Zhang, L. Cao, Z. Q. Wu and X. X. Ma, *J. Mater. Chem. A*, 2022, **10**, 25527-25538.

10 Z. He, J. C. Liu, X. Fan, B. Song and H. B. Gu, *Ind. Eng. Chem. Res.*, 2022, **61**, 17915-17929.